IEEJ Journal of Industry Applications
J-STAGE Advance published date : June 13, 2025
DOI : 10.1541/ieejjia.25000833

Paper

Precise Vibration Measurement with Mechanical Load Isolation for Sub-Fractional Horsepower Motors

Shahin Asgari*,**a) Non-member, Nejat Saed*,** Non-member
Annette Muetze*,** Non-member

(Manuscript received February 03, 2025)

With the increasing use of electric motors as the primary propulsion system in vehicles, vibrations from the main drive have decreased, making those from auxiliary drives more prominent. As a result, addressing audible noise and vibration in the design of auxiliary motors for automotive applications has become increasingly important. These compact drives, often located near passengers, are more audible compared to the main drive system. Consequently, they may produce vibrations that can excite neighboring structures or components, leading to noise-related concerns. Accurately measuring the structure-borne noise of permanent magnet motors presents a significant challenge. This paper introduces an innovative approach to enhance the precision of vibration measurement and differentiate between electromagnetic and mechanical sources of vibration, making it suitable for vibration measurements in sub-fractional horsepower motors. Furthermore, the proposed measurement methodology provides valuable information on the influence of design variations on vibration characteristics.

Keywords: e-NVH, Permanent magnet motors, Sub-fractional horsepower, Vibration measurement

1. Introduction

Electromagnetic forces are a primary source of vibration in electric motors, generating various harmonics that can excite the mechanical structure of the motor[(1)]. The increasing demand for high-performance electric machines has intensified research efforts to optimize the vibration behavior of electric motors, with a particular focus on mitigating electromagnetic vibration sources to enhance acoustic performance. Several studies have investigated the impact of electromagnetic forces on mechanical vibrations in permanent magnet motors as well as magnetic gears. For instance, research on magnetic gears highlights how cogging torque and electromagnetic forces contribute to vibration and noise generation, necessitating advanced modeling techniques such as finite element analysis (FEA) for accurate prediction and mitigation strategies[(2)]. Similarly, in permanent magnet synchronous motors (PMSMs), rotor eccentricity has been identified as a major source of increased radial electromagnetic forces, leading to undesirable mechanical vibrations[(3)]. This phenomenon affects system performance by introducing harmonic distortions that can amplify structural resonance effects. Additionally, in robotic applications, mechanical vibrations in actuators and joints can significantly degrade precision and motion stability. Techniques such as final state control and inertia compensation have been explored to suppress residual vibrations and improve response times[(4)]. Despite these advancements, effectively decoupling mechanical and electrical vibrations remains challenging, particularly in systems where electromagnetic interactions are closely coupled with mechanical dynamics. Yoshiura et al.[(5)] explored a full-closed control system, introducing an anti-resonance vibration suppression technique to overcome limitations caused by anti-resonance frequencies in position feedback systems. Their innovative approach significantly enhanced system stability by effectively suppressing unwanted vibrations. Hara et al.[(6)] addressed electromagnetic noise in PMSMs through synchronous PWM control, strategically shifting carrier wave phases relative to modulated waves. This method neutralized vibration-inducing ripple frequencies caused by space and time harmonics, effectively reducing electromagnetic vibrations. Soeda and Haga[(7)] specifically targeted the suppression of 12th-order torque ripple and radial force vibrations in double-star PMSMs. Through harmonic current superposition, they effectively mitigated both torque ripple and radial vibrations simultaneously, achieving substantial reductions in vibration amplitudes. Rotor eccentricity in PMSMs, a significant source of radial electromagnetic forces, has been extensively studied due to its role in amplifying mechanical vibrations and harmonic distortions[(8)]. Addressing these issues requires precise modeling techniques such as finite element analysis (FEA), which have been increasingly utilized to accurately predict and mitigate vibration-induced effects[(9)].

In a three-phase pulse-width modulation (PWM) inverter, the sum of the phase voltages is inherently nonzero. Consequently, the inverter produces a common-mode (CM) voltage, which can lead to various forms of electromagnetic interfer-

This paper is based on Reference (1), which published in the International Conference ICEMS 2024 ©2024 IEEJ.

a) Correspondence to: s.asgari@tugraz.at
* Electric Drives and Power Electronic Systems Institute, Graz University of Technology, Graz, Austria.
** Christian Doppler Laboratory for Brushless Drives for Pump and Fan Applications ,Graz, Austria.

ence (EMI) within motor drive systems. One notable example is the degradation of motor bearing life due to shaft voltage, potentially causing mechanical vibrations[10]. The order of electromagnetic forces harmonics is related to factors such as synchronous speed, the number of poles and slots, and the excitation method [12], [13]. In small motors, these forces are relatively minor, typically on the order of one hundredth of a Newton, requiring precise measurement methods [14]. Measurement becomes more challenging when vibrations from the load are present, as they intertwine with electromagnetic forces, complicating analysis. To investigate electric motor vibrations, it is essential to understand how design changes impact measurement outcomes. However, this task is complicated further when electromagnetic and mechanical vibrations mix, making it difficult to isolate and evaluate each factor individually.

This paper proposes a method for measuring vibration in sub-fractional horsepower motors, specifically those with an output power of approximately 1 Watt. In such motors, decoupling vibrations caused by the load (e.g., an impeller) or mechanical defects, such as bearing degradation, is challenging during post-processing due to the small amplitude of these forces and the limited repeatability of tests. To overcome this challenge, the proposed method mechanically isolates the motor's load side from the stator. In this configuration, there is no direct mechanical connection between the rotor and the stator, which is the point of vibration measurement. As a result, the only forces transmitted to the measurement point are electromagnetic, precisely the type of forces motor designers aim to evaluate during the design phase. This practical approach allows testing with various loads on a single motor design or comparing different motor designs under a fixed load, facilitating analysis of vibrations attributable solely to electromagnetic forces.

The rest of this article is structured as follows: Section 2 describes the motor structure used as an example to illustrate the proposed vibration measurement method. Section 3 presents both conventional and proposed measurement methods. Section 4 analyzes the measurement results in two scenarios: first, by comparing the conventional and proposed methods, and second, by demonstrating the effectiveness of the proposed method through comparisons of sample cases in healthy and non-healthy conditions arising from manufacturing imperfections. Finally, Section 5 summarizes the findings.

2. The Example Case Motor Structure

The case study is an axial flux permanent magnet (AFPM) motor with a ferrite core using printed circuit board (PCB) winding [15]. This motor is specifically designed to drive a small radial fan for automotive applications, with a rated output power of 1.15 watt. This motor was selected because, in the actual application, the blades are directly connected to the rotor and rotate via the same shaft and bearing as shown in Figure 1. As a result, mechanical and electromagnetic sources of vibrations combine. These combined forces are then transferred either to the structure in real applications or to force sensors for vibration measurements. This makes it an ideal example for investigating both vibration sources together. Figure 2 shows the different parts of the motor, which

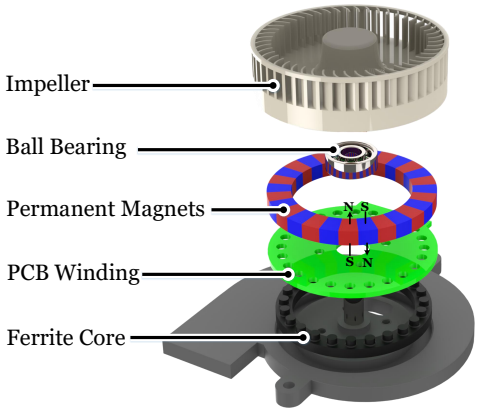

Fig. 1. Exploded view of the case study; The PCB winding motor with a ferrite core.

Fig. 2. Prototyped PCB winding motor components.

comprise a ferrite core, a PCB winding, ferrite magnets, and the impeller. As illustrated, the stator core includes 24 slots, while the rotor has 28 magnet poles. The stator teeth feature a circular cross section, simplifying the assembly process and reducing costs in PCB production. Table 1 presents the motor specifications in detail.

Table 1. The Motor Specifications

Quantity	Units	Values
Rated average output torque	[mN·m]	2.2
Rated power	[W]	1.15
Air-gap length	[mm]	0.3
Number of Pole pairs (p)	[-]	14
Number of slots (Z_s)	[-]	24
Motor axial length	[mm]	10
Motor outer diameter	[mm]	50
Supply voltage	[V]	12.8
Input current peak	[A]	0.162
Rated speed	[rpm]	5000
Magnet thickness	[mm]	4.5
Magnet residual flux density	[mT]	275

The prototype PCB incorporates a multilayer winding structure consisting of eight layers and a total of 24 coils. The winding configuration is divided into three phases, with eight series-connected coils per phase. The phases are connected in a delta configuration. Inter-layer electrical connections are established using vias, allowing current to flow between different PCB layers to complete each coil's geometry. Figure 3 shows the overall winding layout and details the implementation of individual coils within the PCB structure. Each coil is distributed across four PCB layers, with nine turns per layer, resulting in a total of 36 turns per coil. This layered distribution enables a compact winding design while maintaining the required turn count within the limited board area.

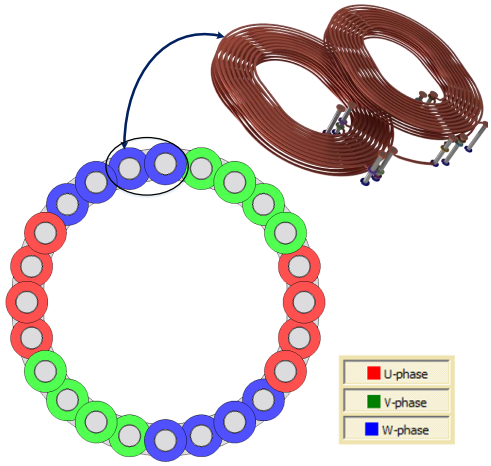

Fig. 3. PCB winding layout showing multi-layer coil structure and phase distribution.

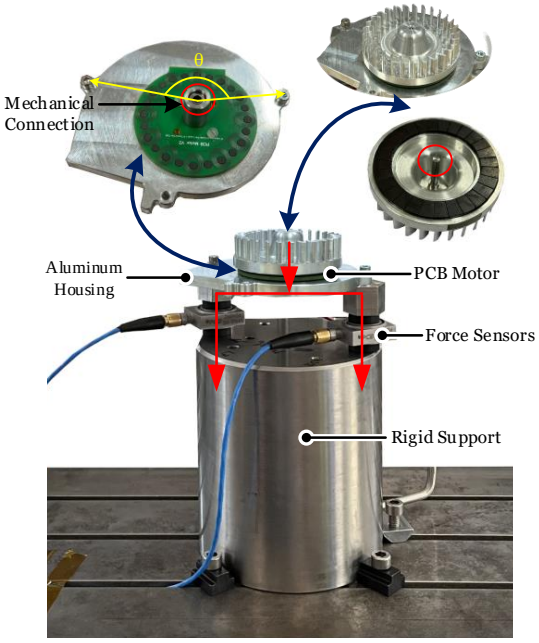

Fig. 4. Conventional vibration measurement setup.

3. Measurement Methods and Setups

3.1 Conventional Vibration Measurement Method

The conventional vibration measurement setup consists of three-axis force sensors and follows the VW 82469 standard [16]. The force sensors are mounted on a stainless steel cylinder, which is decoupled from the bottom support. Due to the cylinder's mass significantly exceeding that of the system, it is considered a rigid abutment according to the standard. The measured data are collected via the 3-channel sound and vibration measurement modules (NI-9232) from National Instruments. As specified in the standard, the measured forces from all attachment points are summed and presented in a one-third octave band analysis. The standard defines three operating limits based on different auxiliary application scenarios commonly found in the automotive industry. These limits distinguish between:

- Auxiliary devices that operate only when the combustion engine is running.
- Devices that can be activated when the engine is off, including those that are automatically triggered when the engine starts.
- Fully automatic auxiliary systems that operate while the engine is off.

Figure 4 illustrates the test bench setup, including the connected fan and force sensors. In this measurement approach, mechanical vibrations-originating from sources such as rotor unbalance or bearing defects are transmitted through the mechanical interfaces shown in Figure 5 and propagate through the motor structure to the sensors. Although it is possible to distinguish these mechanical vibrations from electromagnetic ones during post-processing, complications arise when both types of forces interact within non-linear structural materials. This interaction can obscure the characterization of pure electromagnetic forces. The challenge is especially significant in sub-fractional horsepower motors, where the amplitude of magnetic forces is inherently low, making separation and analysis more difficult.

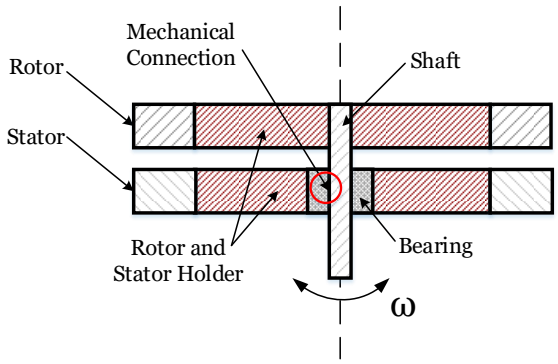

Fig. 5. Cross-sectional view of the motor showing the mechanical connection between the rotor and stator

3.2 Proposed Vibration Measurement Method

To accurately investigate the structural noise behavior of electric motors, it is crucial to evaluate the influence of electromagnetic design parameters on vibration characteristics, thereby providing essential feedback for design optimization and performance enhancement. However, this analysis becomes challenging when electromagnetic vibrations are coupled with mechanical vibration sources, such as rotor unbalance or bearing defects. The proposed measurement method

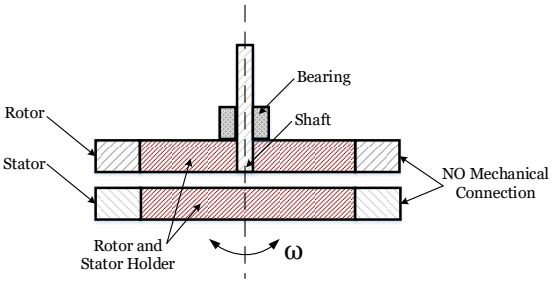

Fig. 6. Cross-sectional view of the motor showing the mechanically isolated rotor and stator.

addresses this issue by mechanically isolating the load from the sensors, thereby reducing the influence of mechanical forces on the measured vibration data and enhancing the reliability of electromagnetic force characterization.

Figure 6 shows a cross-sectional view of the motor, highlighting the absence of any mechanical connection between the rotor and stator. As a result, the measurement point is mechanically isolated from the rotating components.

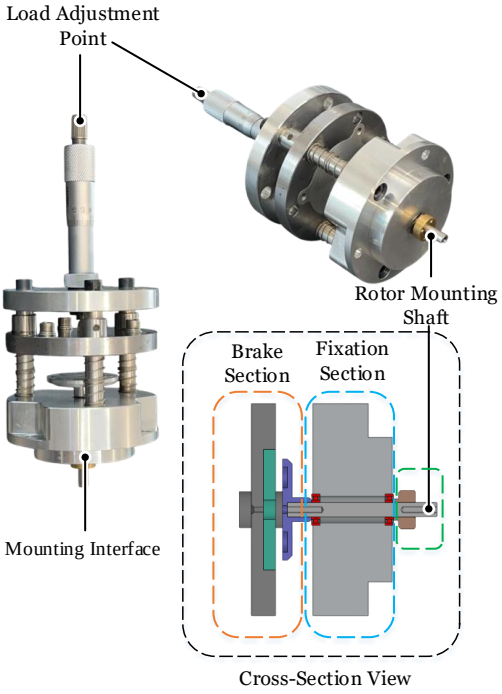

Fig. 7. Eddy current brake used as the motor load, showing cross-sectional view and mounting points.

Figure 7 illustrates the eddy current brake used as a load for the motor. This brake was specifically designed for the experimental setup and selected due to its negligible torque ripple and torque-speed characteristics that closely match the characteristics of a fan load, making it well-suited for this application. Additionally, it offers flexibility in adjusting the load magnitude, enabling testing under various load conditions. As shown in this figure, different rotors can be mounted on the eddy current shaft. The structure of the brake also allows the rotor to be supported and rotated using the bearing located on the eddy current side.

To hold the rotor, the eddy current brake integrated with the rotor is mounted on a supporting structure, as shown in Figure 8. This structure allows precise movement in three directions (X, Y, Z) with a resolution of one-hundredth of a millimeter. The rotor, aligned with the center of the stator, is suspended from the top through its connection to the eddy current brake. The relative positioning between the rotor and stator is achieved through a one-time setup of the holding structure. This position is saved in the controller and reused for all subsequent measurements. The stator remains fixed to the sensors and the stainless steel cylinder, maintaining the

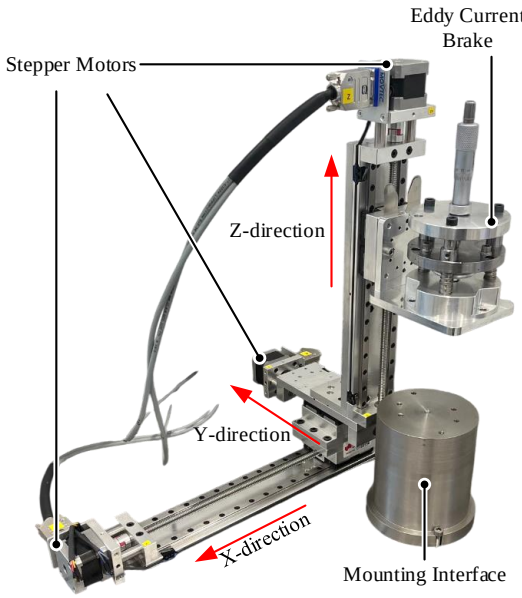

Fig. 8. Holding structure used to mount the rotor and eddy current brake, allowing precise three-axis positioning.

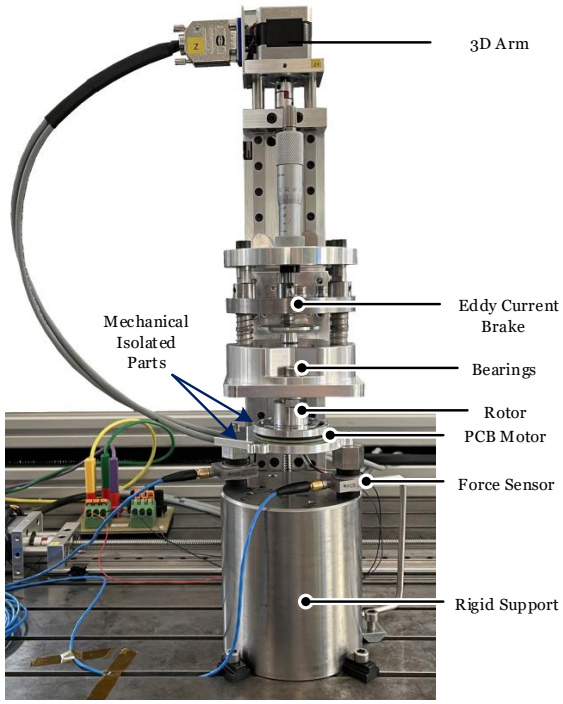

Fig. 9. Proposed vibration measurement setup.

same configuration as in the previous setup.

The final test bench, as shown in Figure 9, integrates all key components necessary for accurate vibration analysis of sub-fractional horsepower motors. The rotor is suspended from the top-mounted eddy current brake. This configuration ensures that only electromagnetic forces are transmitted to the sensor, eliminating the influence of mechanical disturbances such as bearing noise or rotor imbalance. The modular design

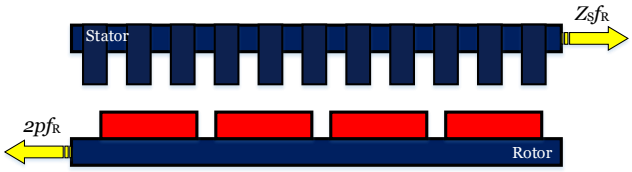

Fig. 10. Teeth and poles passing frequencies.

of the setup also allows for easy replacement or modification of rotor components, making it suitable for a wide range of experimental conditions.

4. Measurement Results and Analyses

Magnetic forces are characterized by amplitude, spatial shape, and frequency. Frequency is an important factor for resonance prediction and is vital for noise, vibration, and harshness (NVH) analysis [17], [18]. This research focuses primarily on the frequency analysis of the forces, as they can significantly excite the components connected to the drive. The force sensors used in the measurement method are capable of detecting forces in a wide range of frequencies. Pulsating forces are, by definition, in phase across both the stator and the rotor. These forces are observed at the same frequency by both the rotor and stator, similar to torque and counter-torque interactions. A rotor pole will inevitably experience variations in magnetic forces at multiples of the stator slot passing frequency, $Z_S f_R$, where Z_S is the number of slots and f_R is the rotor's mechanical rotational frequency. Conversely, a stator tooth experiences variations in magnetic forces at multiples of the pole-passing frequency, $2p f_R$, where $2p$ represents the number of poles, as shown in Fig. 10.

As a result, pulsating forces occur in multiples of the least common multiple (LCM) between $Z_S f_R$ and $2p f_R$ [17]. Therefore, the frequency at which these forces occur is given by:

$$f = LCM(Z_s, 2p) f_R \cdots\cdots\cdots\cdots\cdots\cdots\cdots\cdots\cdots\cdots (1)$$

It should be noted that if there is any asymmetry in the rotor poles and slots, pulsating forces with frequencies of $Z_S f_R$ and $2p f_R$ will appear in addition to the LCM between $Z_S f_R$ and $2p f_R$. In the following subsections, two different scenarios are analyzed to show the accuracy of the proposed measurement method.

4.1 Validation of Measurement Precision Using Defective Components

In this subsection, the vibration behavior of the example case PCB motor with a healthy core and a defective one is compared using the proposed measurement method to prove its capability to detect and distinguish small changes.

Figure 11 shows a microscopic view of one of the core's teeth, which was damaged during the prototyping process. The tooth has a diameter of 3 mm, and the broken section is marked. Although this defect is minor and does not impact the motor's overall performance, it introduces asymmetry in the core. According to the analytical expression at the beginning of Section 4, force at the $2p f_R$ frequency is expected to appear in the measurements. Furthermore, during the prototyping process, segmented rotor magnets were used. Due to manufacturing tolerances, any asymmetry in the pole pairs should result in a force with the frequency of $Z_S f_R$ appearing in the measurement results.

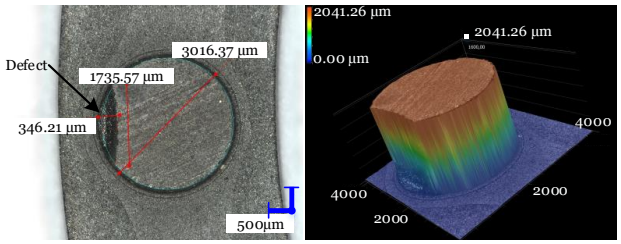

Fig. 11. Microscopic image showing the defective tooth of the motor core..

To investigate the impact of the aforementioned asymmetry on vibration behavior, two tests were performed under identical conditions, with one test using a defective core. The resulting forces were recorded and analyzed using a Fast Fourier Transform (FFT), and the frequency-domain results are presented accordingly.

Figure 12 presents the measured forces along the X, Y, and Z axes for the healthy core configuration. The figure is organized into two columns, with each column representing the data from one sensor and each row corresponding to one of the three force components. It is important to note that if the angular separation between the two sensors (denoted as θ in Figure 4) were exactly 180 degrees, the absolute values of the X- and Y-axis forces would be identical for both sensors. However, in this setup, the mounting angle is slightly less than 180 degrees, which accounts for the differences observed in the X and Y force components measured by the two sensors. To ensure accurate force values, the forces from all measurement points—regardless of the number of sensors or the angle between them—should be summed for each axis (X, Y, and Z). This summation yields reliable results that can be used for meaningful comparison between different test cases.

Figure 13 shows the summed forces derived from the data in Figure 12. As observed, the dominant force component ap-

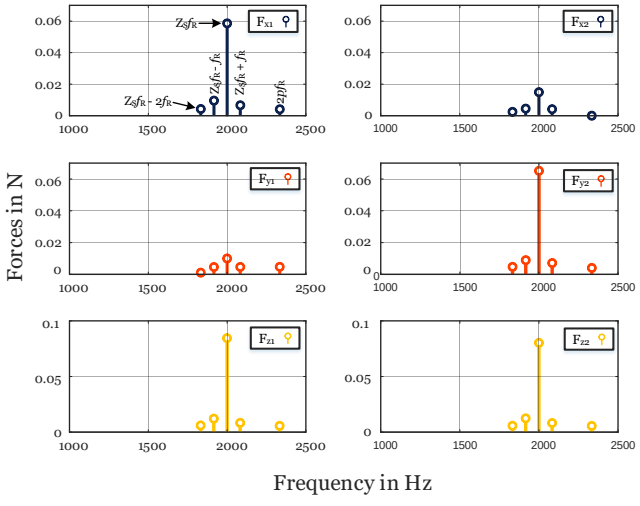

Fig. 12. FFT analysis of forces along all three axes at each measurement point for the healthy core.

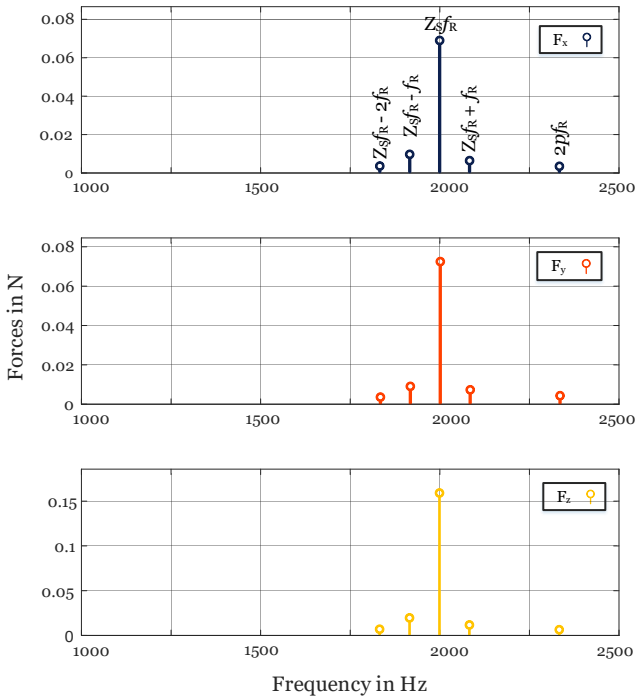

Fig. 13. FFT analysis of forces along all three axes for the healthy core.

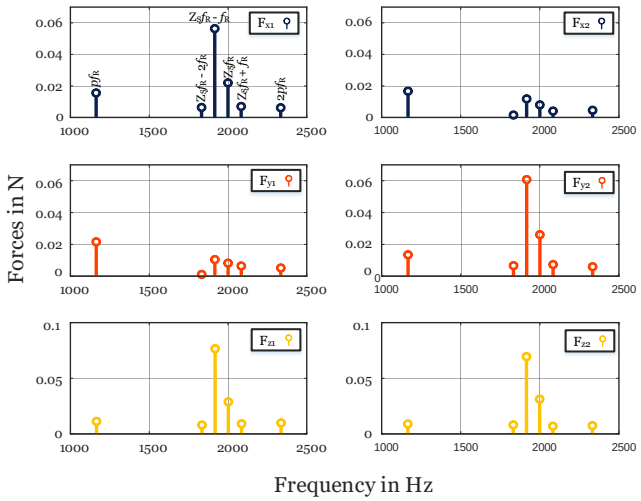

Fig. 14. FFT analysis of forces along all three axes at each measurement point for the defective core.

pears at the $Z_S f_R$ frequency, accompanied by sidebands—an indication of unbalanced electromagnetic forces. The presence of a peak at the $Z_S f_R$ frequency suggests that the rotor poles are not perfectly symmetrical. Although the degree of asymmetry is small, it is successfully detected using the proposed measurement method.

Figure 14 presents the force measurements along all three axes for both sensors in the case of the defective core, while Figure 15 shows the corresponding summed forces.

In addition to the components observed in the healthy core measurements, a distinct force appears at the $p f_R$ frequency. The defect also influences the amplitudes of other frequency components; for example, the amplitude at the $2p f_R$ frequency increases slightly, and a significant rise is observed at the $(Z_s - 1) f_R$ frequency, which is attributed to the presence

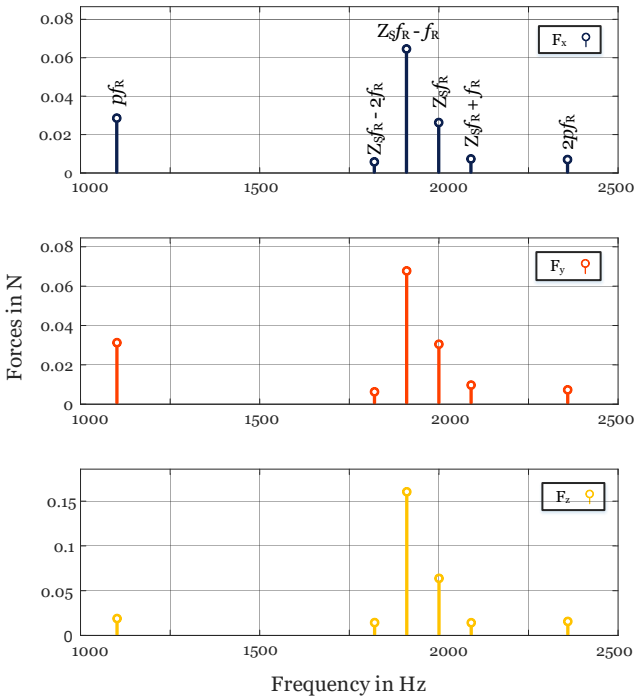

Fig. 15. FFT analysis of forces along all three axes for the defective core.

of a broken tooth. Overall, the vibration spectrum is noticeably affected due to the asymmetry introduced by the defect. The comparison between Figures 13 and 15 validates the accuracy and sensitivity of the proposed measurement method in detecting minor structural changes in the motor.

4.2 Comparison Between Conventional and Proposed Measurement Methods Figure 16 illustrate the measured structure-borne noise in the one-third octave band for the PCB motor using both the conventional and proposed vibration measurement methods, respectively, as described in section three. The motor is excited by a three-phase sinusoidal voltage and operates at 5000 rpm, with a consistent load of 2.2 mN·m applied for both measurement methods. According to the Section 4.1, forces from all attachment points are summed and presented as a one-third octave band spectrum [16].

The primary distinction between these two measurements lies in the type of load and its connection to the measurement points. In the conventional method, the load is a fan that is mechanically connected to the measurement points, allowing both mechanical and electromagnetic forces generated by the rotating parts to influence the measurements. In contrast, the proposed method utilizes an eddy current brake as the load, which has no mechanical connection to the measurement points. This isolation ensures that only electromagnetic forces are transmitted and recorded during measurements, effectively eliminating any interference from mechanical forces caused by rotating components.

The results are plotted on a logarithmic scale for both force and frequency, with the limits represented as three distinct lines. The frequency range is selected up to 1000 Hz, which is typically the most critical range for vibration analysis. The comparison reveals that, across all frequencies, the amplitude of the measured force using the non-isolated method is con-

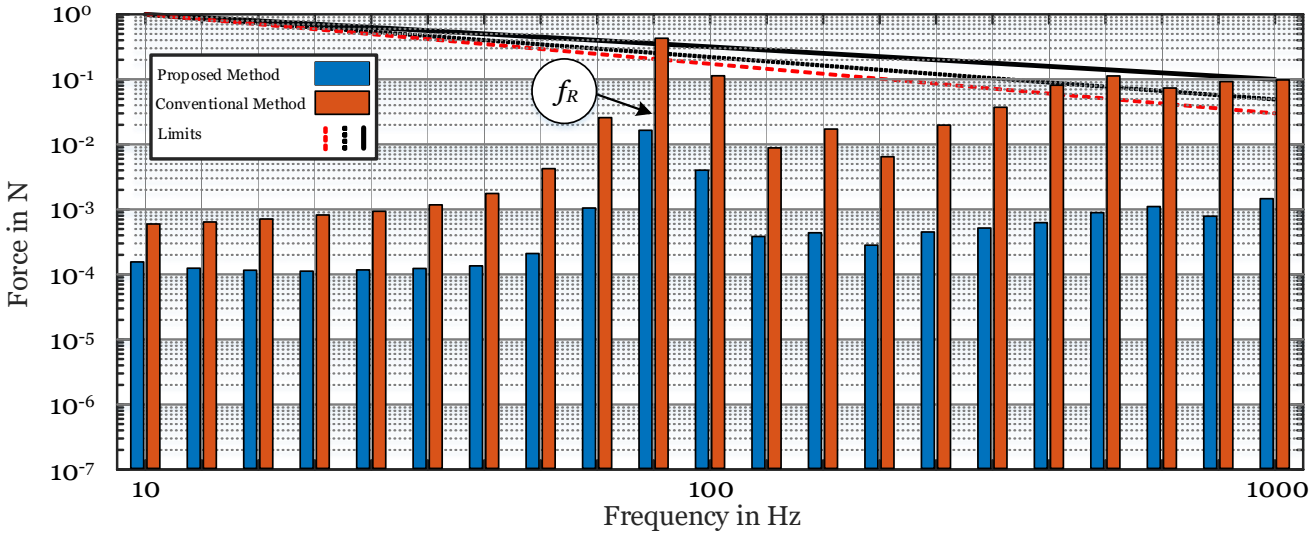

Fig. 16. One-third octave band analysis of structure-borne noise measured using both conventional and proposed methods.

sistently higher than that of the proposed method. In certain frequencies, the amplitude is more than 100 times greater, exceeding the specified limits at six points.
Considering f_R, which is the frequency corresponding to the rotational speed of 5000 rpm, and comparing the forces at this frequency, it becomes evident that the fan experiences mechanical unbalance. While this mechanical issue can be disregarded during the analysis as a non-electromagnetic source, it is important to note that the amplitudes of all other forces across different frequencies are influenced by this unbalance. Moreover, if there is a bearing issue or a fan with varying levels of unbalance, it can alter the force signatures. These problems are particularly pronounced in sub-fractional horsepower motors, where the absolute force values are very small and can be easily affected.

All of these uncertainties complicate the replication of measurement results and make it challenging for motor designers to concentrate on structure-borne noise caused by electromagnetic forces. In contrast, with the proposed method, the sensors exclusively measure electromagnetic forces, resulting in considerably more accurate and repeatable outcomes.

5. Conclusions

This study presents a novel vibration measurement method tailored for sub-fractional horsepower motors, offering a significant improvement in the accuracy of electromagnetic force characterization. By mechanically isolating the rotor and load from the stator and sensors, the proposed approach eliminates interference from mechanical disturbances such as rotor imbalance and bearing imperfections. This enables a more precise evaluation of electromagnetic forces, which are critical for NVH assessments in compact motor designs.

The findings have direct practical implications for motor designers and engineers. The proposed setup provides a repeatable and interference-free environment to evaluate the vibrational impact of design changes. This allows designers to optimize rotor and stator geometries with a higher degree of confidence, leading to quieter and more reliable motor design,—particularly important in automotive auxiliary applications where audible noise is a growing concern.

Future work will involve validating the proposed approach through finite element simulations and comparing these results with measured data. Additionally, the method can be extended to evaluate the influence of other factors such as winding topology, core geometry, and thermal expansion on vibration characteristics. Ultimately, this work lays the foundation for a standardized measurement approach that supports the development of low-noise, cost-effective electric drives.

Acknowledgment

This work was supported in part by the Austrian Federal Ministry of Labor and Economy, and in part by the National Foundation for Research, Technology, and Development and the Christian Doppler Research Association.

The authors would like to express their gratitude to Dr. Markus Mosshammer and MSG Mechatronic Systems GmbH, Wies, Austria, for their support in manufacturing the test bench components. Special thanks are also extended to Ing. Christoph Schmidt and Keyence International, Austrian Branch, Vienna, Austria, for providing the microscopic images of the parts.

References

(1) S. Asgari, N. Saed, and A. Muetze. Precise Vibration Measurement with Mechanical Load Isolation for Sub-Fractional Horsepower Motors. In 27th International Conference on Electrical Machines and Systems (ICEMS2024-Fukuoka), Fukuoka, Japan, November 2024.

(2) N. Niguchi, K. Hirata, and A. Zaini. Electromagnetic Vibration Analysis and Measurement of a Magnetic Gear. *IEEJ Journal of Industry Applications*, vol. 2, no. 6, pp. 261–268, 2013. doi: 10.1541/ieejjia.2.261.

(3) R. Takahata, S. Wakui, K. Miyata, K. Noma, and M. Senoo. Influence of Rotor Eccentricity on Vibration Characteristics of Permanent Magnet Synchronous Motor. *IEEJ Journal of Industry Applications*, vol. 8, no. 3, pp. 558–565, 2019. doi: 10.1541/ieejjia.8.558.

(4) T. Yoshioka, N. Shimada, K. Ohishi, T. Miyazaki, and Y. Yokokura. Vibration Suppression Control based on Final State Control Considering Convergence Time and Inertia Variation for Industrial Robot. *IEEJ Journal of Industry Applications*, vol. 3, no. 3, pp. 236–247, 2014. doi: 10.1541/ieejjia.3.236.

(5) Y. Yoshiura, Y. Asai, and Y. Kaku. Anti-resonance Vibration Suppression Control in Full-closed Control System. *IEEJ Journal of Industry Applications*, vol. 9, no. 3, pp. 311–317, 2020. doi: 10.1541/ieejjia.9.311.

(6) T. Hara, T. Tsukagoshi, S. Taniguchi, and T. Ajima. Vibration Reduction of Permanent Magnet Synchronous Motor Driven by Synchronous PWM Control with Carrier Wave Phase Shifts. *IEEJ Journal of Industry Applications*, vol. 11, no. 2, pp. 379–387, 2022. doi: 10.1541/ieejjia.20012660.

(7) T. Soeda and H. Haga. Twelfth-order Vibration Suppression Strategy for Double-Star PMSM. *IEEJ Journal of Industry Applications*, vol. 14, no. 1, pp. 133–134, 2025. doi: 10.1541/ieejjia.L24000622.

(8) K. Yang, K. Akatsu, K. Okazaki, and Y. Miyama. Imbalanced Force Suppression Due to Static Eccentricity by using Triple Three-phase Winding Motor. *IEEJ Journal of Industry Applications*, vol. 12, no. 4, pp. 763–772, 2023. doi: 10.1541/ieejjia.22008991.

(9) Y. Bo, S. Li, and G. Hu. Research on electromagnetic force wave analysis and vibration characteristics of permanent magnet synchronous motor based on finite element simulation. In *2020 IEEE 3rd International Conference of Safe Production and Informatization (IICSPI)*, pp. 192–196, 2020. doi: 10.1109/IICSPI51290.2020.9332464.

(10) S. Takahashi and S. Maekawa. Attenuation Characteristics of the Input/Output Coupling Passive EMI Filter on Conducted Emission in Motor Drive Systems. *IEEJ Journal of Industry Applications*, vol. 11, no. 5, pp. 709–710, 2022. doi: 10.1541/ieejjia.L21001373.

(11) K. Yang and K. Akatsu. Vibration Suppression of a Specific Harmonic Component by Teeth Flux Density Control Using Multi-Phase MATRIX Motor. *IEEJ Journal of Industry Applications*, vol. 12, no. 2, pp. 194–203, 2023. doi: 10.1541/ieejjia.22008707.

(12) J. F. Gieras, C. Wang, and J. C. Lai, Noise of Poly-phase Electric Motors. Boca Raton: CRC Press, 2017.

(13) P. L. Timar, Noise and Vibration of Electrical Machines. Elsevier, 1989.

(14) N. Saed, S. Asgari, and A. Muetze. Vibration Analysis of Single-Phase Brushless DC Fan Drives Considering Position Signal Error. IEEE Transactions on Industry Applications, vol. 60, no. 4, pp. 6242–6251, Jul. 2024.

(15) S. Asgari, N. Saed, and A. Muetze. Low-Cost Axial Flux PCB Motor with Ferrite Core and Ferrite Magnet Topology for Fan Applications. In 2023 IEEE International Electric Machines and Drives Conference (IEMDC2023-San Francisco), San Francisco, CA, USA, May 2023.

(16) F. Bielert, Zusatzaggregate - Akustische Anforderungen, Volkswagen Konzernnorm. VW 82 469.

(17) Noise control of electrical machines, Solutions for noise and vibration control of electrical systems. Accessed: Aug. 31, 2024. [Online]. Available: https://e-nvh.eomys.com/

(18) W. Li et al.. Structural Analysis of Single-Sided Axial-Flux Permanent Magnet Machines With Different Magnetic Materials. IEEE Transactions on Magnetics, vol. 57, no. 2, pp. 1–5, Feb. 2021.

Shahin Asgari (Non-member) received the M.S. degree from the Amirkabir University of Technology (AUT), Tehran, Iran, in 2015 in electrical engineering. He worked for four years as a researcher at the Electrical Machines and Transformers Research Laboratory (EMTRL) at Amirkabir University of Technology in Tehran, Iran. He is currently pursuing his Ph.D. degree in electrical engineering at the Electric Drives and Power Electronic Systems Institute at the Graz University of Technology, Graz, Austria. His research interests include auxiliary drive and traction motor design, analysis, and optimization for automotive applications.

Nejat Saed (Non-member) received the B.S. and M.S. degrees both in electrical engineering from Shahid Beheshti University, Tehran, Iran, and Amirkabir University of Technology (Tehran Polytechnic), Tehran, Iran, in 2015 and 2018, respectively. He is currently pursuing his Ph.D. degree in electrical engineering at the Electric Drives and Power Electronic Systems Institute at the Graz University of Technology, Graz, Austria. His main research interests include design and prototyping of electric drives, analysis, modeling and optimization of PM electric machines and power electronics.

Annette Muetze (Non-member) received the Dipl.-Ing. and the Dr.-Ing. degrees in electrical engineering from Darmstadt University of Technology, Darmstadt, Germany, in 1999 and 2004, respectively, and the Diploma in general engineering from the Ecole Centrale de Lyon, Ecully, France, in 1999. Since 2010, she has been a Full Professor at Graz University of Technology, Graz, Austria. Before joining the Graz University of Technology, she was an Assistant Professor with the University of Wisconsin-Madison, Madison, WI, USA, and an Associate Professor with the University of Warwick, Coventry, U.K. She has also been the head of Senate of TU Graz since summer 2022.